# Ray Curvature on a Flat Earth for Computing Virtual WSR-88D Signatures of Simulated Supercell Storms

ROBERT DAVIES-JONES[a] AND VINCENT T. WOOD

*NOAA/National Severe Storms Laboratory, Norman, Oklahoma*

MARK A. ASKELSON

*Department of Atmospheric Sciences, University of North Dakota, Grand Forks, North Dakota*

(Manuscript received 5 October 2018, in final form 18 December 2018)

ABSTRACT

Two accepted postulates for applications of ground-based weather radars are that Earth's surface is a perfect sphere and that all the rays launched at low-elevation angles have the same constant small curvature. To accommodate a straight vertically launched ray, we amend the second postulate by making the ray curvature dependent on the cosine of the launch angle. A standard atmospheric stratification determines the ray-curvature value at zero launch angle. Granted this amended postulate, we develop exact formulas for ray height, ground range, and ray slope angle as functions of slant range and launch angle on the real Earth. Standard practice assumes a hypothetical equivalent magnified earth, for which the rays become straight while ray height above radar level remains virtually the same function of the radar coordinates. The real-Earth and equivalent-earth formulas for height agree to within 1 m. Our ultimate goal is to place a virtual Doppler radar within a numerical or analytical model of a supercell and compute virtual signatures of simulated storms for development and testing of new warning algorithms. Since supercell models have a flat lower boundary, we must first compute the ray curvature that preserves the height function as the earth curvature tends to zero. Using an approximate height formula, we find that keeping planetary curvature minus the ray curvature at zero launch angle constant preserves ray height to within 5 m. For standard refraction the resulting ray curvature is negative, indicating that rays bend concavely upward relative to a flat earth.

## 1. Introduction

The radar-measurable variables that identify a target's position are slant range, which is calculated from the time delay between transmitted and received pulses, the elevation angle of the radar ray at the radar antenna (hereafter called the launch angle), and the azimuth angle of the ray. Hence, the radar coordinates, which are intrinsic to data collection, are slant range $r$ (arc length along a stationary ray), azimuth $\beta$, and launch angle $\alpha$. Important quantities not measured directly but derived from the radar variables are ray height above radar level, ground range, and ray slope angle.

Accepted postulates for applications of ground-based weather radars are (i) that the surface of the Earth[1] is a perfect sphere level with the radar antenna and (ii) that the rays are circular with constant curvature (typically much less than Earth curvature). A standard atmospheric stratification determines the value of the ray curvature (Doviak and Zrnić 2006, 19–21; Petrocchi 1982). As pointed out by Askelson (2002), postulate (ii) excludes the straight vertically launched ray. Here we amend postulate (ii) by allowing ray curvature to vary with the cosine of the launch angle. Granted this amended postulate, we develop exact formulas for the derived variables as functions of slant range and launch angle. These formulas are constrained by the properties of a vertically

[a] Emeritus.

*Corresponding author*: Vincent T. Wood, vincent.wood@noaa.gov

[1] We use the proper noun "Earth" in reference to the actual Earth, and the common noun "earth" when referring to a fictitious earth such as a flat earth or equivalent earth.

DOI: 10.1175/MWR-D-18-0356.1

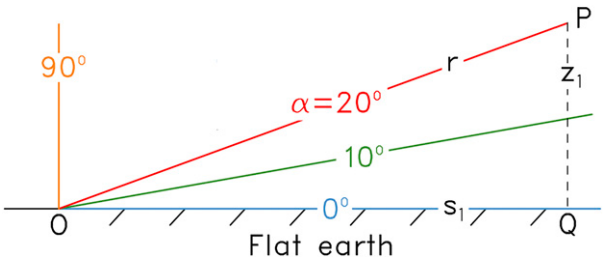


FIG. 1. Schematic illustrating straight rays launched at angles 0° (blue), 10° (green), 20° (red), and 90° (orange) in an azimuthal-vertical plane over a flat earth surface (hatched). In this case there is no atmospheric refraction. The radar antenna is at O and P is a measurement point at slant range $r$ and height $z_1$ on a ray launched at an angle $\alpha = 20°$; Q is the surface point on the vertical line through P (dashed black line). It is at ground range OQ = $s_1$. The ground surface coincides here with the tangent plane so $H_1 = z_1$ and $\Sigma_1 = s_1$.

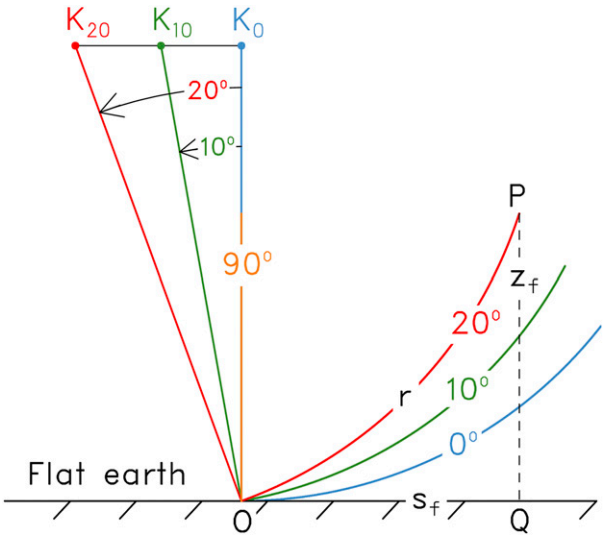


FIG. 2. As in Fig. 1, but for negatively curved (concave upward, $\kappa_f < 0$) rays over a flat earth. The vertically launched ray is straight. The ground and tangent plane are coincident so $H_f = z_f$, the height QP of P, and $\Sigma_f = s_f$, the ground range OQ. $K_0$, $K_{10}$, and $K_{20}$ are the centers of curvature and $K_0O$, $K_{10}O$, and $K_{20}O$ are radii for circular rays launched from the radar O at angles $\alpha = 0°$, 10°, and 20°, respectively. According to (8) with $\kappa_f < 0$ the centers of curvature all lie in a plane parallel to and above the ground. The slant range $r$ of P is the arc length OP. The rays' negative curvatures are chosen to force the heights of the rays above the flat earth and the heights of positively curved rays over the actual Earth with standard atmospheric refraction to closely approximate the same functions of slant range and launch angle.

launched ray. At a launch angle of 90°, the formulas satisfy the correct conditions of zero ray curvature, zero ground range, constant ray slope angle of 90°, and equality of slant range and height.

Assuming a flat earth instead of a spherical one and ignoring atmospheric refraction (case 1, Fig. 1) yields simple formulas that are sufficient for ranges only up to a few tens of kilometers (Xu and Wei 2013). At longer ranges serious height errors occur owing to absence of both earth curvature and ray curvature. For computing the signatures of simulated storms with a virtual Doppler radar, keeping the model's flat earth and calculating an adjusted ray curvature, which preserves the height function (i.e., the dependence of height on slant range and launch angle) to an excellent approximation, is the most practical approach (case 2, Fig. 2). Standard practice, following Schelleng et al. (1933), postulates an equivalent magnified earth, for which the rays become straight (case 3, Fig. 3). Keeping the relative curvature (the planetary curvature minus a constant ray curvature) invariant determines the radius of the equivalent earth. Schelleng et al. demonstrated that for nearly horizontal rays the equivalent-earth model closely replicated results from their real-Earth model. Note however that, unlike the equivalent-earth model, their real-Earth model cannot imitate a vertically launched ray or rays with considerable slopes. For atmospheric observations, we can retain the real-Earth curvature and assume ray curvature that varies with the cosine of the launch angle (case 4, Fig. 4). This provides us with formulas for the actual Earth that are correct for the vertically launched straight ray and agree very closely with those of the equivalent-earth model. The invariant quantity is now the relative curvature *evaluated at zero launch angle*. Thus, we can derive from our real-Earth model the adjusted ray curvature required in a flat-earth model to preserve the height function.

In section 2 we derive exact solutions for ray height, ground range, and ray slope angle as functions of slant range and launch angle. These solutions are exact only as far as the amended postulates are true. Section 3 tailors these solutions to specific geometries, namely flat earth, equivalent earth, and actual Earth. At this stage the radius of the equivalent earth and the ray curvature to be used on a flat earth are unspecified. In section 4 we find an approximate solution for ray height that is accurate to within 7 m for ranges up to 250 km. This solution depends on the curvatures only via the relative curvature of a ray launched horizontally. This relationship enables us to find the appropriate ray curvature for a flat earth and the radius of an equivalent earth that retain the same function for height versus slant range and launch angle as on the real Earth. Section 5 contains sample calculations in the different cases of height, ground range, and slope angle for slant ranges and launch angles that span the values used by operational WSR-88Ds on thunderstorm days [this span is evident in Fig. 1 of Xu and Wei (2013)]. We present conclusions and planned future work in section 6.

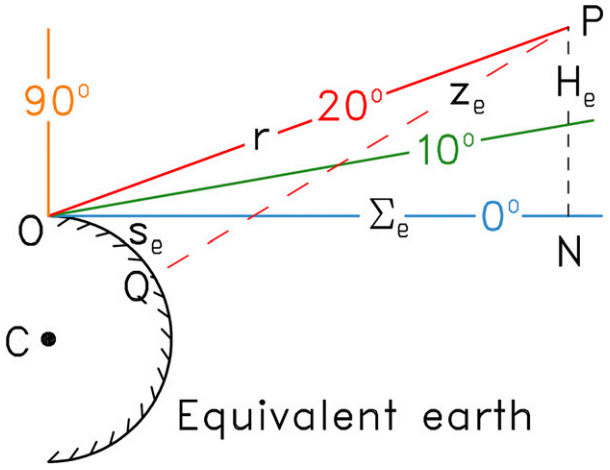


FIG. 3. Hypothetical straightened rays launched at angles $\alpha = 0°$ (blue), 10° (green), 20° (red), and 90° (orange) from a radar antenna at O on an enlarged equivalent earth (cross-hatched) with center at C; P is a measurement point on a ray launched at an angle $\alpha = 20°$. The slant range $r$ is the straight-line distance from O to P. The red, long-dashed line PQ is the vertical through P to the ground point Q. The length of QP is the height $z_e$ of P. The length OQ measured along the surface of the equivalent earth is the ground range $s_e$. The tangent plane at O is coincident with the $\alpha = 0°$ surface. The length NP of the perpendicular from P to the tangent plane at N is $H_e$ and the distance of N from the radar at O is $\Sigma_e$. The radius $a_e$ of the equivalent earth is chosen so that the heights of the straight rays and the heights of positively curved rays over the actual Earth with standard atmospheric refraction are very nearly the same functions of slant range and launch angle.

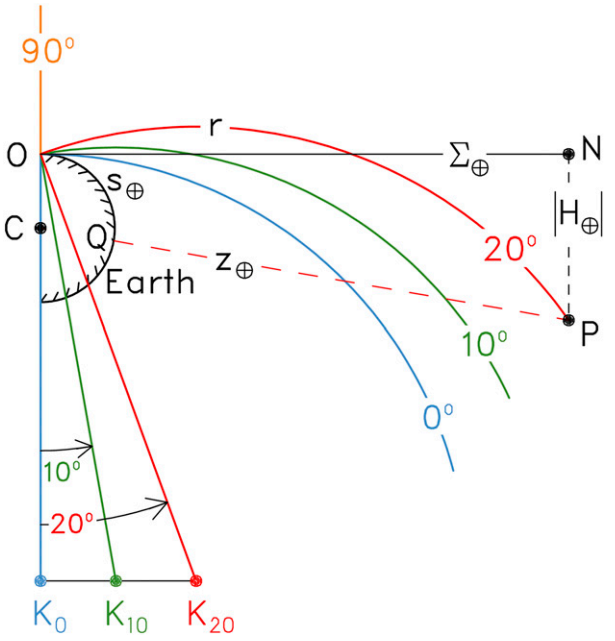


FIG. 4. Positively curved rays ($\kappa_\oplus > 0$) launched at a given azimuth angle from a radar antenna at O on the real Earth (cross-hatched) with center at C. The diagram is drawn to scale for standard refraction but the rays (circular arcs apart from the straight orange vertically launched ray) are unrealistically long for purposes of illustration. $K_0$, $K_{10}$, and $K_{20}$ are the centers of curvature and $K_0O$, $K_{10}O$, and $K_{20}O$ are the radii for the blue, green, and red rays launched at angles $\alpha = 0°$, 10°, and 20°, respectively. Owing to the amended postulate, the centers of curvature all lie in a plane specified by (8). This plane is parallel to and below the tangent plane at O because the ray curvature is positive. P is a measurement point on a ray launched at an angle $\alpha = 20°$. The slant range $r$ is the arc length along the ray from O to P. The red, long-dashed straight line PQ is the vertical through P to the surface point Q. The length of QP is the height $z_\oplus$ of P. The length OQ measured along the surface of the Earth is the ground range $s_\oplus$ of P. NP is the perpendicular from P to the tangent plane ON. The length of NP is $H_\oplus$ (<0 in this diagram since P is below the tangent plane) and the distance ON is $\Sigma_\oplus$.

## 2. Ray geometry and height

As customary (Doviak and Zrnić 2006, 18–23), we assume that the planetary surface is a sphere with radius $a$ equal to the distance from the planet's center C to the radar antenna at O and that a ray has constant curvature $\kappa$ owing to refraction by the atmosphere. Subscripts $\oplus$, $f$, and $e$ pertain to actual-Earth, flat-earth, and equivalent-earth values, respectively, and the term "planet" refers to either the real Earth ($a_\oplus \approx 6371$ km), or a flat earth ($a_f \approx \infty$) as assumed in supercell models, or a hypothetical equivalent earth (of radius $a_e = 1.21a_\oplus$, see section 4), for which the rays under standard refraction are straightened. The curvature $\kappa$ is positive (negative) if the ray is concave downward (upward). From Doviak and Zrnić [2006, their Eq. (2.24a)], an approximate formula for ray curvature is

$$\kappa = \frac{-dn/dz}{\left[1 + (dz/ds)^2\right]^{1/2}}, \tag{1}$$

where $z$ is height above antenna level, $s$ is ground range from the antenna, and $n(z)$ is refractive index in a typical spherically stratified atmosphere. Doviak and Zrnić assume that $n$ is a linear function of height and that elevation angles are small so that $(dz/ds)^2$ is negligible. Under these conditions all rays are circular arcs with the same curvature. Here we depart from the approximation of small elevation angle by assuming that $dz/ds$ is approximately equal to $\tan\alpha$. Thus,

$$\kappa = \kappa_0 \cos\alpha, \tag{2}$$

where $\kappa_0 \equiv -dn/dz$ is the curvature of rays launched at $\alpha = 0°$. In this approximation, all nonvertical rays are still arcs of circles but the curvature varies from ray to ray according to the cosine of launch angle.

We use two coordinate systems, Cartesian coordinates associated with the tangent plane at the radar and right-handed curvilinear nonorthogonal coordinates that are radar-measured position identifiers. The position vector in the Cartesian system is $\mathbf{X} \equiv X\mathbf{i} + Y\mathbf{j} + H\mathbf{k}$ where $\mathbf{i}, \mathbf{j}, \mathbf{k}$

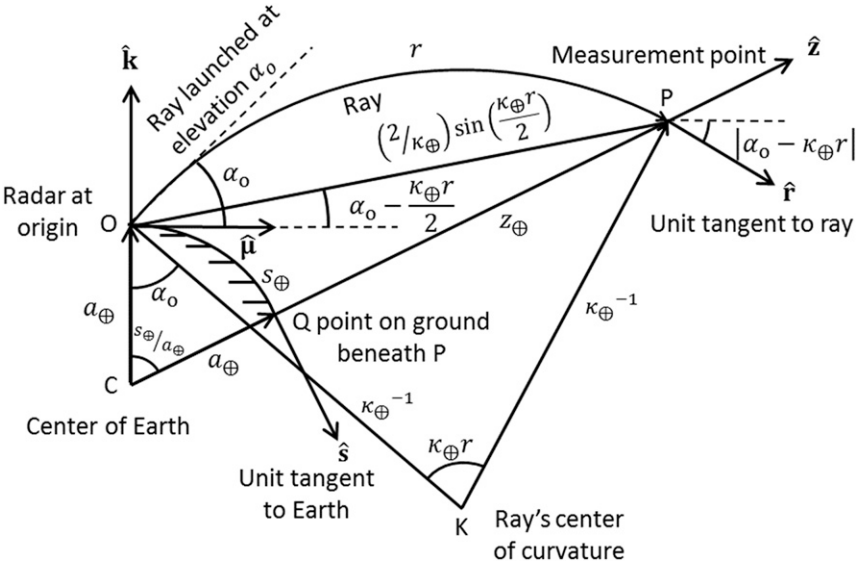


FIG. 5. Geometry of a ray launched from a radar at O at azimuthal angle $\beta$ and elevation angle $\alpha$ to a general measurement point P($r$, $\alpha$, $\beta$). The ray follows the circular arc OP of arc length $r$, radius $1/\kappa_\oplus$ = KO = KP, and center of curvature K. The Earth's surface, assumed spherical, is cross-hatched; Q is the point on the Earth's surface vertically below P; $z_\oplus$ = PQ is the height of P; $s_\oplus$ is the ground range (distance from O to Q along the Earth's surface); $a_\oplus$ = CO = CQ is the Earth's radius; and C is the center of the Earth. The ray turns through an angle $\kappa_\oplus r$ between O and P so the ray's elevation angle at P relative to the tangent plane at O is $\alpha - \kappa_\oplus r$ (depicted $< 0$). Its elevation angle relative to the local horizontal at Q is $\alpha + s_\oplus/a_\oplus - \kappa_\oplus r$ where $s_\oplus/a_\oplus = \angle$OCP. The chord OP subtends an angle $\kappa_\oplus r$ at K so its length is $(2/\kappa_\oplus)\sin(\kappa_\oplus r/2)$. Since KOP is an isosceles triangle, $\angle$KOP $= \pi/2 - \kappa_\oplus r/2$. The depression angle of KO is $\pi/2 - \alpha$ and so the elevation angle of OP is $\alpha - \kappa_\oplus r/2$, both relative to the tangent plane at O. The unit vectors (all in the ray's azimuthal plane unless otherwise noted) are $\mathbf{k}$, the local vertical at O; $\hat{\boldsymbol{\mu}} \equiv \sin\beta\,\mathbf{i} + \cos\beta\,\mathbf{j}$, the local horizontal at O; $\mathbf{u}_3$ (not shown) $\equiv \cos\beta\,\mathbf{i} - \sin\beta\,\mathbf{j}$, the unit vector normal to the azimuthal plane; $\hat{\mathbf{r}} = \cos(\alpha - \kappa_\oplus r)\,\hat{\boldsymbol{\mu}} - \sin(\alpha - \kappa_\oplus r)\,\mathbf{k}$, the tangent to the ray at P; $\hat{\mathbf{s}} = \cos(s_\oplus/a_\oplus)\,\hat{\boldsymbol{\mu}} - \sin(s_\oplus/a_\oplus)\,\mathbf{k}$, the tangent to the Earth at Q; and $\hat{\mathbf{z}} = \sin(s_\oplus/a_\oplus)\,\hat{\boldsymbol{\mu}} + \cos(s_\oplus/a_\oplus)\,\mathbf{k}$, the upward vertical at P.

form an orthonormal basis with **i** eastward, **j** northward, and **k** upward at the radar antenna O. Note that these fixed vectors are either parallel or normal to the tangent plane at O and do not follow the planetary surface if it is curved. Consider a measurement point P and its projection N onto the tangent plane. The Cartesian coordinate $H$ of P is the height of P above the tangent plane and the coordinates $X$ and $Y$ are, respectively, east and north distances to N from the radar. The curvilinear coordinates ($r$, $\alpha$, $\beta$) are based on the geometry of the radar ray. The origin is at the radar antenna O and $r$ is the slant range (defined as arc length distance from O along a ray to the measurement point P), $\alpha$ is the launch angle of the ray, and $\beta$ is the ray azimuth angle measured clockwise from due north. Angles are measured in radians unless stated otherwise.

Figure 5 illustrates the geometry of an individual radar ray relative to the planet. In a plane of constant azimuth $\beta$, the ray's center of curvature is at K and the position vector **X** of a measurement point P is a chord OP of the ray's circular path with length $(2/\kappa)\sin(\kappa r/2)$ [Askelson 2002, his Eq. (2.3)]. The elevation angle of the chord relative to the tangent plane is $\alpha - \kappa r/2$. The equation of a stationary ray ($\alpha$ = const. and $\beta$ = const.) parameterized by arc length distance $r$ from the radar is therefore

$$\mathbf{X}(r,\alpha,\beta) = X\,\mathbf{i} + Y\,\mathbf{j} + H\,\mathbf{k} = \Sigma\hat{\boldsymbol{\mu}} + H\,\mathbf{k}, \qquad (3)$$

where

$$\begin{aligned} H(r,\alpha) &= \frac{2}{\kappa}\sin\left(\frac{\kappa r}{2}\right)\sin\left(\alpha - \frac{\kappa r}{2}\right), \\ \Sigma(r,\alpha) &= \frac{2}{\kappa}\sin\left(\frac{\kappa r}{2}\right)\cos\left(\alpha - \frac{\kappa r}{2}\right), \\ X(r,\alpha,\beta) &= \Sigma(r,\alpha)\sin\beta, \\ Y(r,\alpha,\beta) &= \Sigma(r,\alpha)\cos\beta, \end{aligned} \qquad (4)$$

defines ($X$, $Y$, $H$) in terms of the radar coordinates ($r$, $\alpha$, $\beta$). Here $\Sigma = (X^2 + Y^2)^{0.5}$ is distance in the tangent plane and the unit vector $\hat{\boldsymbol{\mu}} \equiv \sin\beta\,\mathbf{i} + \cos\beta\,\mathbf{j}$ is along the ray's azimuth. Use of trigonometric identities gives us the alternative formulation

$$\mathbf{X}(r,\alpha,\beta) = \Sigma(r,\alpha)\hat{\boldsymbol{\mu}}(\beta) + H(r,\alpha)\mathbf{k}$$
$$= \left(\frac{\sin\kappa r}{\kappa}\cos\alpha + \frac{1-\cos\kappa r}{\kappa}\sin\alpha\right)\hat{\boldsymbol{\mu}}(\beta)$$
$$+ \left(\frac{\sin\kappa r}{\kappa}\sin\alpha - \frac{1-\cos\kappa r}{\kappa}\cos\alpha\right)\mathbf{k}. \quad (5)$$

Since $|\kappa r| << 1$ and $\cos\kappa r$ is very nearly 1, we should always compute $1 - \cos\kappa r$ using the equivalent expression $2\sin^2(\kappa r/2)$. From (5) it is evident that

$$\Sigma = \frac{\sin\kappa r}{\kappa}\cos\alpha + \frac{1-\cos\kappa r}{\kappa}\sin\alpha,$$
$$H = \frac{\sin\kappa r}{\kappa}\sin\alpha - \frac{1-\cos\kappa r}{\kappa}\cos\alpha \quad (6)$$

in the cases in Figs. 2 and 4, for which $\kappa \neq 0$. For the cases in Figs. 1 and 3, we take the limit as $\kappa \to 0$ and thus obtain

$$\Sigma = r\cos\alpha, \quad H = r\sin\alpha. \quad (7)$$

The center of curvature K of a ray is at

$$(\Sigma, H)_K = \frac{1}{\kappa}(\sin\alpha, -\cos\alpha) = \frac{1}{\kappa_0}(\tan\alpha, -1) \quad (8)$$

owing to (2). Thus, the centers of curvature all lie in a plane parallel to the tangent plane $H = 0$ (see Figs. 2, 4). The separation distance of the two planes is equal to the radii of those rays that are launched horizontally.

Given the Cartesian coordinates of points in a numerical or analytical model we may wish to obtain their radar curvilinear coordinates. This is done as follows. Let $R = (\Sigma^2 + H^2)^{0.5}$ be the straight-line distance of P from O. Then it follows from (4) that

$$R = \frac{2}{\kappa}\sin\frac{\kappa r}{2}, \quad (9)$$

$$H = R\sin\left(\alpha - \frac{\kappa r}{2}\right). \quad (10)$$

From (10), (9), and (4),

$$\alpha = \sin^{-1}\frac{H}{R} + \sin^{-1}\frac{\kappa R}{2}, \quad (11)$$

$$r = \frac{2}{\kappa}\sin^{-1}\frac{\kappa R}{2} \quad \text{if} \quad \kappa \neq 0,$$
$$= R \quad \text{if} \quad \kappa = 0 \quad (12)$$

$$\beta = \sin^{-1}\frac{X}{\Sigma} \quad \text{and} \quad \cos^{-1}\frac{Y}{\Sigma}. \quad (13)$$

In cases 2 and 4 where $\kappa = \kappa_0\cos\alpha \neq 0$, we solve (11) for $\alpha$ by Newton's method.

A ray launched at zero elevation angle and refracted with the planet's curvature $1/a$, follows the planet's surface. Thus, we obtain the equation of the planet's surface from (4) and (5) by setting $\alpha = 0$ and replacing $\kappa$ with $1/a$ and $r$ with $s$, the ground range OQ (measured along the planet's surface). Therefore, the position vectors $\mathbf{Y}(s, \beta)$ of points on the surface are

$$\mathbf{Y}(s,\beta) = a\sin\frac{s}{a}\hat{\boldsymbol{\mu}} + a\left(\cos\frac{s}{a} - 1\right)\mathbf{k}. \quad (14)$$

The unit tangent to the planet in the direction of increasing $s$ at constant azimuth is

$$\hat{\mathbf{s}} \equiv \frac{\partial\mathbf{Y}}{\partial s} = \cos\frac{s}{a}\hat{\boldsymbol{\mu}} - \sin\frac{s}{a}\mathbf{k}, \quad (15)$$

and the one in the direction of increasing $\beta$ with constant $s$ is

$$\mathbf{u}_3 = \frac{d\hat{\boldsymbol{\mu}}}{d\beta} = \cos\beta\,\mathbf{i} - \sin\beta\,\mathbf{j}. \quad (16)$$

The unit outward normal to the planet is

$$\hat{\mathbf{z}} \equiv \mathbf{u}_3 \times \hat{\mathbf{s}} = \sin\frac{s}{a}\hat{\boldsymbol{\mu}} + \cos\frac{s}{a}\mathbf{k}. \quad (17)$$

The position vector $\mathbf{Z}$ from O of a measurement point P on a vertical at height $z$ above the planet's surface is equal to the position vector of C from O plus the position vector of P from C (see Fig. 5). In other words,

$$\overrightarrow{\mathrm{OP}} = \overrightarrow{\mathrm{OC}} + \overrightarrow{\mathrm{CP}} \Rightarrow$$
$$\mathbf{Z} = -a\mathbf{k} + (a+z)\hat{\mathbf{z}}. \quad (18)$$

The equation of a vertical is therefore

$$\mathbf{Z}(s,\beta,z) = (a+z)\sin\frac{s}{a}\hat{\boldsymbol{\mu}} + \left[(a+z)\cos\frac{s}{a} - a\right]\mathbf{k}. \quad (19)$$

As $a \to \infty$ (cases 1 and 2),

$$\mathbf{Z} \to s\hat{\boldsymbol{\mu}} + z\mathbf{k} \quad (20)$$

Since (5) and (19) evaluated at P both provide the position vector of P, we require that

$$\Sigma\hat{\boldsymbol{\mu}} + H\,\mathbf{k} = \begin{cases} (a+z)\sin\frac{s}{a}\hat{\boldsymbol{\mu}} + \left[(a+z)\cos\frac{s}{a} - a\right]\mathbf{k} & \text{in cases 3 and 4} \\ s\hat{\boldsymbol{\mu}} + z\mathbf{k} & \text{in cases 1 and 2} \end{cases} \quad (21)$$

By equating components in (21) we find in cases 1 and 2

$$s = \Sigma, \quad z = H. \tag{22}$$

Similarly, we obtain in cases 3 and 4

$$\Sigma = (a + z)\sin\frac{s}{a}, \tag{23}$$

$$a + H = (a + z)\cos\frac{s}{a}. \tag{24}$$

By eliminating $a + z$ from (23) and (24) we obtain

$$s(r,\alpha) = a\tan^{-1}\frac{\Sigma}{a + H} \tag{25}$$

and by adding the square of (23) to the square of (24) and solving for $z$ we get

$$z(r,\alpha) = [(a + H)^2 + \Sigma^2]^{1/2} - a. \tag{26}$$

Relative to the local horizontal, the slope angle $\theta$ of a ray at a data point P equals the launch angle plus the angle that the planet's surface turns through from the radar at O to the surface point Q beneath P minus the angle of refraction that the ray bends through from O to P. Thus, the ray slope angle is

$$\theta = \alpha + \frac{s}{a} - \kappa r. \tag{27}$$

For computing the signatures of simulated storms with a virtual Doppler radar, $(s, \alpha, \beta)$ coordinates are more convenient than $(r, \alpha, \beta)$ since $s$ is readily available and $r$ is not. Let P be a point at a given ground range on a specific ray identified by its launch angle and azimuth. We require the slant range of P in order to compute the height of P and the ray's slope angle at P in order to compute Doppler velocity. Thus, we need in the various cases the inverse relationships for the slant range $r$ as a function of the ground range $s$ and launch angle $\alpha$. These are obtained in the appendix.

## 3. Compiling the formulas for each case

We now assemble the formulas for each case from the equations in section 2 and the appendix. In the trivial case 1 (Fig. 1) of a flat earth with no atmospheric refraction (denoted by subscript 1), the height, slant range-ground range relationships and the ray slope angle are simply

$$\begin{aligned} &z_1 = H_1 = r\sin\alpha, \quad s_1 = \Sigma_1 = r\cos\alpha, \\ &r = s_1/\cos\alpha, \quad \theta_1 = \alpha. \end{aligned} \tag{28}$$

For case 3, which is no refraction on an equivalent earth (denoted by subscript $e$), we have from (7), (25)–(27), and (A3),

$$\Sigma_e = r\cos\alpha, \quad H_e = r\sin\alpha, \tag{29}$$

$$s_e = a_e\tan^{-1}\frac{r\cos\alpha}{a_e + r\sin\alpha}, \tag{30}$$

$$z_e = a_e\left(1 + \frac{2r}{a_e}\sin\alpha + \frac{r^2}{a_e^2}\right)^{1/2} - a_e. \tag{31}$$

$$\theta_e = \alpha + s_e/a_e, \tag{32}$$

$$r = \frac{a_e\sin(s_e/a_e)}{\cos(\alpha + s_e/a_e)} \tag{33}$$

(see Fig. 3). We find the $a_e$ of the equivalent earth in section 4. Case 3 approaches case 1 in the limit as $a_e \to \infty$.

For flat-earth geometry (case 2, Fig. 2), we set $\kappa = \kappa_f$ where subscript $f$ denotes flat and let $1/a \to 0$. The modified ray curvature for a flat earth is determined in section 4. Figure 6 depicts the geometry of the radar beam over a flat earth. For this geometry the ground coincides with the tangent plane so $z_f = H_f$ and $s_f = \Sigma_f$. In a plane of constant azimuth $\beta_0$, the ray's center of curvature is at K and the position vector $\mathbf{x} \equiv x\mathbf{i} + y\mathbf{j} + z\mathbf{k}$ of a measurement point P is a chord OP of the ray's circular path with length $(2/\kappa_f)\sin(\kappa_f r/2)$. The elevation angle of the chord relative to the earth's surface is $\alpha - \kappa_f r/2$. For a flat earth, it is evident from Fig. 6 or from (6), (22), (27), and (A8) that

$$s_f = \Sigma_f = \frac{\sin\kappa_f r}{\kappa_f}\cos\alpha + \frac{1 - \cos\kappa_f r}{\kappa_f}\sin\alpha, \tag{34}$$

$$z_f = H_f = \frac{\sin\kappa_f r}{\kappa_f}\sin\alpha - \frac{1 - \cos\kappa_f r}{\kappa_f}\cos\alpha, \tag{35}$$

$$\theta_f = \alpha - \kappa_f r, \tag{36}$$

$$r = \frac{1}{\kappa_f}[\alpha + \sin^{-1}(\kappa_f s_f - \sin\alpha)]. \tag{37}$$

As $\kappa_f \to 0$, (34)–(37) tend to the case 1 formulas in (28).

In case 4 (Figs. 4, 5) for the real Earth (denoted by subscript $\oplus$) we have from (6), (25)–(27), and (A7)

$$\Sigma_\oplus = \frac{\sin\kappa_\oplus r}{\kappa_\oplus}\cos\alpha + \frac{1 - \cos\kappa_\oplus r}{\kappa_\oplus}\sin\alpha, \tag{38}$$

$$H_\oplus = \frac{\sin\kappa_\oplus r}{\kappa_\oplus}\sin\alpha - \frac{1 - \cos\kappa_\oplus r}{\kappa_\oplus}\cos\alpha, \tag{39}$$

$$s_\oplus = a_\oplus\tan^{-1}\frac{\Sigma_\oplus}{a_\oplus + H_\oplus}, \tag{40}$$

$$z_\oplus = [(a_\oplus + H_\oplus)^2 + \Sigma_\oplus^2]^{1/2} - a_\oplus, \tag{41}$$

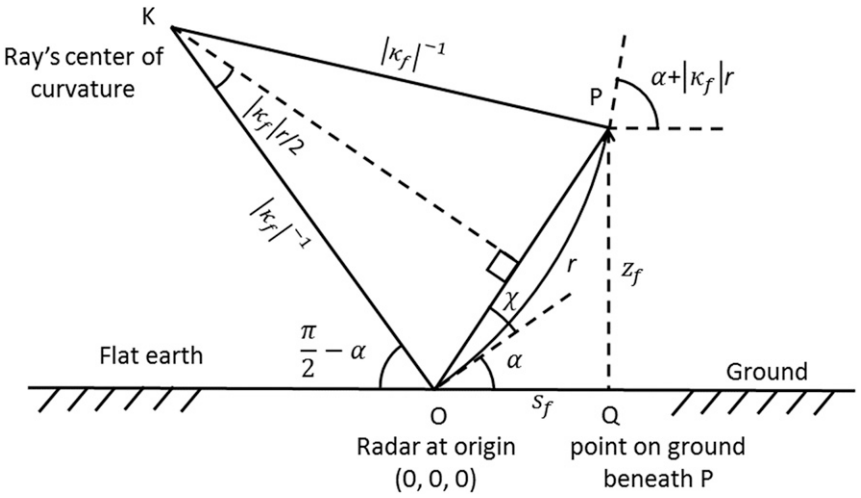


FIG. 6. As in Fig. 5, but for a flat earth ($1/a_f = 0$). The curvature $\kappa_f$ is negative so the ray is now concave upward. The angle OKP = the slant range $r$ divided by the radius of curvature $1/|\kappa_f|$. Since OKP is an isosceles triangle, the length of the chord OP is $(2/\kappa_f)\sin(\kappa_f r/2)$. The angle $\chi$ is the angle between the chord OP and the tangent to the ray at O. Since the four separate angles at O add up to $\pi$, $\chi = \pi - (\pi/2 - \alpha) - (\pi/2 - |\kappa_f|\, r/2) - \alpha = |\kappa_f|\, r/2$. Therefore, the elevation angle of the position vector OP is $\alpha - \kappa_f r/2$ (since $\kappa_f < 0$). The height of P is $z_f = \mathrm{OP}\sin(\alpha + \chi) = (2/\kappa_f)\sin(\kappa_f r/2)\sin(\alpha - \kappa_f r/2)$ and its ground range is $s_f = (2/\kappa_f)\sin(\kappa_f r/2)\cos(\alpha - \kappa_f r/2)$. The ray turns through the angle $|\kappa_f|\, r$ so the beam slope angle at P is $\alpha - \kappa_f r$.

$$\theta_\oplus = \alpha + \frac{s_\oplus}{a_\oplus} - \kappa_\oplus r, \tag{42}$$

$$r = \frac{1}{\kappa_\oplus}\left\{\alpha + \frac{s_\oplus}{a_\oplus} + \sin^{-1}\left[a_\oplus \kappa_\oplus \sin\frac{s_\oplus}{a_\oplus} - \sin\left(\alpha + \frac{s_\oplus}{a_\oplus}\right)\right]\right\}. \tag{43}$$

Note that taking the limit as $a \to \infty$ in (38)–(43) yields the flat-earth formulas (34)–(37) (with change of subscript). Similarly, (38)–(42) revert to the equivalent-earth counterparts (29)–(32) in the limit as $\kappa \to 0$. [Although (43) does not tend obviously to (33) in this limit, it is a result of (A5) which does, as shown in the appendix.]

## 4. Parameter determination

We make small angle approximations in this section to find the equivalent curvatures that preserve the height function approximately across different planet geometries. First note that in case 1 there are no curvature parameters to adjust to reach agreement with the real-Earth case 4. Consequently, this model greatly underestimates the beam height at long range. Its slope angle is an inaccurate estimate as it does not vary from the launch angle.

Obtaining the following approximate formula for height reveals how to adjust curvatures for different geometries. For typical ray curvatures $\kappa_\oplus r$ is a small quantity since it is less than $10^{-2}$ for ranges up to 250 km. Thus we may approximate $\sin\kappa_\oplus r$ by $\kappa_\oplus r$ and $1 - \cos\kappa_\oplus r$ by $(\kappa_\oplus r)^2/2$ in (38) and (39), which become

$$\begin{aligned} \Sigma_\oplus &\approx r\cos\alpha + \kappa_\oplus r^2 \sin\alpha/2, \\ H_\oplus &\approx r\sin\alpha - \kappa_\oplus r^2 \cos\alpha/2. \end{aligned} \tag{44}$$

Substituting (44) into (41) produces

$$\frac{z}{a_\oplus} \approx -1 + \left[1 + \frac{2r}{a_\oplus}\sin\alpha + \frac{r^2}{a_\oplus^2}\left(1 - a_\oplus\kappa_\oplus\cos\alpha + \cancel{\frac{\kappa_\oplus^2 r^2}{4}}\right)\right]^{1/2}. \tag{45}$$

where the crossed out term is negligible. Askelson (2002) derived a height formula [his (2.4c)] that is equivalent to (45). By series expansion in $r/a$ (<0.04)

$$\frac{z}{a_\oplus} = \frac{r}{a_\oplus}\sin\alpha + \frac{r^2}{2a_\oplus^2}(1 - a_\oplus\kappa_\oplus\cos\alpha - \sin^2\alpha) + \mathrm{O}\left(\frac{r^3}{a_\oplus^3}\right). \tag{46}$$

Thus, an approximate formula for height on the real Earth is

$$z_a \approx r\sin\alpha + \frac{r^2\cos^2\alpha}{2}\left(\frac{1}{a_\oplus} - \kappa_0\right), \tag{47}$$

where we have used (2) and the subscript $a$ denotes approximate. For rays launched at elevation angles greater than 60° and measurement points at heights less than 16 km above radar level (with resultant slant ranges less than 19 km) the second term on the right of (47) is less than 6 m. Thus, the height becomes practically independent of the curvatures at large $\alpha$. In particular, for a ray launched vertically $z_a = r$ as it should. For operational launch angles, the approximate ray height depends on $a_\oplus$ and $\kappa_0$ only in the combination $1/a_\oplus - \kappa_0$, which is the Earth's curvature minus the curvature of a ray launched horizontally. This enables the definition of an equivalent earth of radius $a_e$ on which the radar beams are straight ($\kappa_e = 0$) and the ray height is virtually the same as on the real Earth. The required curvature of the equivalent earth is

$$\frac{1}{a_e} = \frac{1}{a_\oplus} - \kappa_0 \tag{48}$$

(Table 1). For refraction in the U.S. standard atmosphere $a_e = 4a_\oplus/3$ (Doviak and Zrnić 2006, p. 21), which requires $\kappa_0 = 1/(4a_\oplus)$ according to (48). Here we adopt the standard refraction formula used by the Open Radar Product Generator of the WSR-88D (NEXRAD) radar network (Stumpf et al. 2005). In this formula $a_e = 1.21a_\oplus$ (Petrocchi 1982), which by (48) corresponds to $\kappa_0 = 1/(5.76a_\oplus)$ for our use in the exact formulas in section 2.

On a flat earth the ray curvature $\kappa_f$ that keeps the ray curvature at zero launch angle minus the planetary curvature invariant and thus preserves the height-slant range relationship is

$$\kappa_f = \left(\kappa_0 - \frac{1}{a_\oplus}\right)\cos\alpha = \left(\frac{1}{5.76} - 1\right)\frac{\cos\alpha}{a_\oplus} \tag{49}$$

(see Table 1). Since $\kappa_f < 0$ the rays are concave upward (Xu and Wei 2013). Table 1 summarizes the curvature formulas for the different earths.

We now have a way to investigate the dependence of vortex signatures on range. Our method utilizes a Doppler-radar simulator to obtain at different ranges the Doppler-velocity patterns either of simple analytical vortex flows (e.g., Davies-Jones and Wood 2006)[2] or of velocity fields produced in a numerical simulation of a supercell above a flat lower boundary (Wood et al. 2018). Formula (49) provides ray curvature as a function of launch angle $\alpha$. We use the relationship (37) [or (A8)] to determine arc lengths $r$ along rays at specified ground ranges $s$. We then use (35) to compute the heights of ray points. From (36) we calculate the ray slope angles that are needed in calculations of Doppler velocities.

TABLE 1. Planetary curvature $1/a$ and ray curvature $\kappa_0 \cos\alpha$ under conditions of standard NEXRAD refraction for the real Earth (radius $a_\oplus \approx 6.371 \times 10^6$ m, case 4), for an equivalent earth (case 3), and for a flat earth (case 2). In case 1 the earth is flat and there is no refraction. In cases 2, 3, and 4 the planetary curvature minus the ray curvature at 0° launch angle (i.e., $1/a - \kappa_0$) is invariant to keep beam height the same function of slant range. For refraction in the U.S. standard atmosphere instead of standard refraction, replace 1/5.76 with 1/4.

| | Planetary curvature ($m^{-1}$) | Ray curvature ($m^{-1}$) |
|---|---|---|
| Case 4: Real Earth, standard refraction | $1/a_\oplus$ | $\cos\alpha/(5.76a_\oplus)$ |
| Case 3: Equivalent earth, no refraction | $(1-1/5.76)/a_\oplus$ | 0 |
| Case 2: Flat earth, standard refraction | 0 | $-\cos\alpha\ (1-1/5.76)/a_\oplus$ |
| Case 1: Flat earth, no refraction | 0 | 0 |

## 5. Results

In the volume coverage patterns used by operational WSR-88D weather radars to scan thunderstorms, the launch angle $\alpha$ varies from 0.5° to 19.5° and the slant range $r$ extends to around 250 km. The paired values $(r, \alpha)$ in Tables 2–4 represent observation points on the lowest ray and near the tops of storms.

We performed calculations with double precision (15 significant digits) rather than single precision (7 significant digits) so that we could compute small differences in height accurately. Recall from section 2 that for accurate computation $1 - \cos\kappa r$ should be replaced everywhere by the equivalent expression $2\sin^2(\kappa r/2)$. Table 2 shows, for the selected values of $r$ and $\alpha$, the height in the equivalent-Earth model, which is the one in standard use, and the deviations from this height in models with different geometries. The height error in case 1 (flat earth, no refraction) is excessive [as depicted in Fig. 1 of Xu and Wei (2013) or computed from Table 2]. For example, it is 4 km at 250 km range. The approximate height, which pertains collectively to cases 2, 3, and 4, deviates from the equivalent-Earth height by at most 7 m. Height in the real-earth model (case 4) differs from that in the equivalent-Earth model by no more than 1 m. Height on the flat earth (case 2) deviates from equivalent-Earth height by at most 4 m. The height differences in cases 2 to 4 decrease rapidly with inverse range and are trivial

[2] In Eq. (6) of Davies-Jones and Wood (2006), $2\pi$ should have been $r$.

TABLE 2. Ray height $z_e$ on the equivalent earth, calculated from (31), for selected values of slant range $r$ and launch angle $\alpha$ that are chosen to approximate the extent of slant ranges and elevation angles used by operational WSR-88D radars on thunderstorm days. Also shown are the deviations from $z_e$ of (i) $z_\oplus$, the exact height on the real Earth calculated from (41), (ii) $z_f$, the height over a flat earth calculated from (35), and (iii) $z_a$, the approximate height on the real Earth calculated from (47). The height error in case 1 is $z_e$ (column 3) $- r \sin\alpha$ (column 7). The approximate height $z_a$ is the sum of the three terms in the last three columns. The calculated radius of the equivalent earth and the designed ray curvature over a flat earth correspond to ray curvature $\kappa_\oplus = \cos\alpha/(5.76a)$ over the real Earth.

| $r$ (km) | $\alpha$ (°) | $z_e$ (m) | $z_\oplus - z_e$ (m) | $z_f - z_e$ (m) | $z_a - z_e$ (m) | $r \sin\alpha$ (m) | $+r^2\cos^2\alpha/2a$ (m) | $-\kappa_0 r^2 \cos\alpha/2$ (m) |
|---|---|---|---|---|---|---|---|---|
| 250 | 2.4 | 14 509 | −1 | 4 | 7 | 10 469 | 4896 | −850 |
| 250 | 0.5 | 6232 | 0 | 1 | 2 | 2182 | 4905 | −851 |
| 125 | 6.2 | 14 499 | 0 | 1 | 2 | 13 500 | 1212 | −210 |
| 125 | 0.5 | 2104 | 0 | 0 | 0 | 1091 | 1226 | −213 |
| 100 | 8.7 | 15 758 | 0 | 1 | 1 | 15 126 | 767 | −133 |
| 100 | 0.5 | 1521 | 0 | 0 | 0 | 873 | 785 | −136 |
| 50 | 19.5 | 16 834 | 0 | 0 | 0 | 16 690 | 174 | −30 |
| 50 | 0.5 | 598 | 0 | 0 | 0 | 436 | 196 | −34 |

compared to half of the half-power beamwidth of a WSR-88D (roughly 400 m at 50 km range and 2 km at 250 km). Since 0° is a possible supplemental launch angle being tested currently at two WSR-88Ds, we also calculated the height differences in cases 2–4 for zero launch angle and ranges of 50, 100, 125, and 250 km. These differences were 1 m or less.

Table 2 also lists the three terms in the approximate-height formula (47). The first term applies to straight beams ($\kappa_0 = 0$) on a flat Earth ($a = \infty$), the second term is the large correction for Earth curvature, and the third term is a smaller but still significant correction for atmospheric refraction.

Table 3 lists deviations in cases 2–4 of ground range $s$ from $r\cos\alpha$, which is the ground range $s_1$ in case 1 (flat earth, no refraction). The deviations increase with planetary curvature. However, the maximum deviation in the table is just slightly more than 0.2% of $r\cos\alpha$. Using (28), (37), (33), and (A7) in cases 1–4, respectively, recovers slant range from ground range to well within a meter.

TABLE 3. Slant range $r$ times cos $\alpha$ minus ground range $s$ for selected values of slant range $r$ and launch angle $\alpha$ and for different planet geometries. Here $s_\oplus$, $s_e$, $s_f$, and $s_1$ are the ground ranges on the real Earth, on the equivalent earth, on the flat earth with standard refraction, and on the flat earth without refraction. Note that $r\cos\alpha - s_1 \equiv 0$. Formulas (40), (30), (34), and (28) supply $s_\oplus$, $s_e$, $s_f$, and $s_1$, respectively.

| $r$ (km) | $\alpha$ (°) | $r\cos\alpha - s_\oplus$ (m) | $r\cos\alpha - s_e$ (m) | $r\cos\alpha - s_f$ (m) |
|---|---|---|---|---|
| 250 | 2.4 | 470 | 426 | 213 |
| 250 | 0.5 | 175 | 158 | 79 |
| 125 | 6.2 | 252 | 228 | 114 |
| 125 | 0.5 | 32 | 29 | 14 |
| 100 | 8.7 | 220 | 199 | 100 |
| 100 | 0.5 | 19 | 17 | 8 |
| 50 | 19.5 | 113 | 102 | 51 |
| 50 | 0.5 | 4 | 4 | 2 |

The beam slope angle $\theta$ is essential for computing virtual Doppler velocity from model wind fields. Since $s \approx r\cos\alpha$ (Table 3),

$$\theta \approx \alpha + r\cos\alpha\left(\frac{1}{a_\oplus} - \kappa_0\right) \tag{50}$$

from (27) and (2). Thus keeping the planetary curvature minus the ray curvature at 0° launch angle invariant

TABLE 4. Beam slope angle $\theta$ for selected values of slant range $r$ and launch angle $\alpha$ and for different planet geometries (real Earth, equivalent earth, flat earth with standard refraction). For flat earth with no refraction $\theta = \alpha$. In general $\theta = \alpha + s/a - \kappa r$ where the terms $s/a$ and $-\kappa r$ are listed for each geometry.

| $r$ (km) | $\alpha$ (°) | Earth/earth | $+s/a$ (°) | $-\kappa r$ (°) | $\theta$ (°) |
|---|---|---|---|---|---|
| 250 | 2.4 | Real | +2.241 | −0.3899 | 4.2522 |
| | | Equivalent | +1.8533 | −0 | 4.2533 |
| | | Flat | +0 | +1.8565 | 4.2565 |
| 250 | 0.5 | Real | +2.2466 | −0.3902 | 2.3565 |
| | | Equivalent | +1.8569 | −0 | 2.3569 |
| | | Flat | +0 | +1.8580 | 2.3580 |
| 125 | 6.2 | Real | +1.1153 | −0.1940 | 7.1214 |
| | | Equivalent | +0.9219 | −0 | 7.1219 |
| | | Flat | +0 | +0.9236 | 7.1236 |
| 125 | 0.5 | Real | +1.1238 | −0.1951 | 1.4287 |
| | | Equivalent | +0.9288 | −0 | 1.4288 |
| | | Flat | +0 | 0.9290 | 1.4290 |
| 100 | 8.7 | Real | +0.8870 | −0.1543 | 9.4327 |
| | | Equivalent | +0.7332 | −0 | 9.4332 |
| | | Flat | +0 | +0.7347 | 9.4347 |
| 100 | 0.5 | Real | +0.8891 | −0.1561 | 1.2430 |
| | | Equivalent | +0.7431 | −0 | 1.2431 |
| | | Flat | +0 | +0.7432 | 1.2432 |
| 50 | 19.5 | Real | +0.4229 | −0.0736 | 19.8493 |
| | | Equivalent | +0.3495 | −0 | 19.8495 |
| | | Flat | +0 | +0.3503 | 19.8503 |
| 50 | 0.5 | Real | +0.4496 | −0.0780 | 0.8716 |
| | | Equivalent | +0.3716 | −0 | 0.8716 |
| | | Flat | +0 | +0.3716 | 0.8716 |

preserves the slope angle well. For a flat earth with no refraction, the slope angle is just the launch angle. This differs from the real-Earth slope angle by almost 2° at 250 km range. In cases 2–4, the slope angles are the same to a tolerance of 0.005° (Table 4). The cosines and sines of these slope angles differ insignificantly (by less than 0.0001). Table 4 also illustrates that the ray-curvature and earth-curvature terms in the expression for slope angle maintain nearly the same sum to make the slope angle practically the same on the flat earth, the equivalent earth and the real Earth (cases 2–4).

## 6. Summary

Given the assumptions that the earth's surface is a perfect sphere of radius $a_\oplus$ through the antenna and that the radar rays have curvature $\kappa_\oplus$ that varies only with the cosine of the launch angle (our real-Earth model), we obtain exact formulas for ray height (41), ground range (40), and beam slope angle (42) as functions of slant range $r$ and launch angle $\alpha$. We find that the heights given by the equivalent-earth model agree with our real-Earth heights to within 1 m for the volume coverage patterns used by WSR-88Ds in thunderstorm situations. We demonstrate that to an excellent approximation ray height is the same function of slant range if planetary curvature minus ray curvature at zero launch angle is held constant. This allows us to formulate a flat-earth model in which ray curvature is adjusted to compensate for zero earth curvature. The ray curvature for the flat-earth model is provided by (49). With standard refraction ray height varies from real Earth to flat earth by 6 m at most. The ray curvature is negative for standard refraction, indicating that rays bend concavely upward relative to a flat earth. The beam slope angle is virtually the same in the real-Earth, the equivalent-earth, and flat-earth models. Ground range in the flat-earth model differs from its value on the real earth because the geometrical transformation to a flat earth distorts space. However, even at long range (250 km), the deviation is only around 250 m, which is the range gate resolution of a WSR-88D. For a virtual radar inserted in a supercell model, the slant range $r$ is a latent variable and we can regard the ground range $s_f$ as an observed variable. Thus, we trace a ray launched at an angle $\alpha$ by using (37) to derive $r$ from $s_f$, then finding the height and slope angle of the ray from (35) and (36).

Planned work involves placing a virtual Doppler radar within a numerical or analytical model of a supercell with a flat lower boundary, and computing the virtual signatures of simulated storms, using the ray curvatures derived herein. Varying the radar location will enable us to investigate effects of range and viewing direction on the magnitudes of various signatures.

*Acknowledgments.* The authors thank Dr. Dusan Zrnić, Dr. Qin Xu and the three anonymous reviewers for their valuable comments and suggestions that improved the paper. Thanks are also due to Walter Zittel, Richard Murnan, and Daniel Berkowitz of National Weather Service Radar Operation Center Applications Branch for assisting in providing reference information (e.g., Petrocchi 1982) on the index of refraction in the computation of beam height.

## APPENDIX

### Retrieving Slant Range from Ground Range

By rearranging (25), inserting (6), and using a trigonometric identity, we get

$$a\sin\frac{s}{a} = \Sigma\cos\frac{s}{a} - H\sin\frac{s}{a} = \frac{\sin\kappa r}{\kappa}\cos\Lambda + \frac{1-\cos\kappa r}{\kappa}\sin\Lambda, \quad \text{(A1)}$$

where $\Lambda \equiv \alpha + s/a$. For cases 1 and 3, (A1) becomes in the limit as $\kappa \to 0$

$$r\cos\Lambda = a\sin\frac{s}{a}. \quad \text{(A2)}$$

Therefore, in case 3 (equivalent earth) where $a = a_e$ and $\kappa \to 0$,

$$r = \frac{a_e\sin(s_e/a_e)}{\cos(\alpha + s_e/a_e)}. \quad \text{(A3)}$$

In case 1 where $a \to \infty$ and $\kappa \to 0$ (flat earth, no refraction), (A3) reduces to

$$r = s_1/\cos\alpha. \quad \text{(A4)}$$

When $\kappa \neq 0$ (cases 2 and 4), we can multiply both sides of (A1) by $\kappa$ and write it in the form

$$\cos\Lambda\sin\kappa r - \sin\Lambda\cos\kappa r = a\kappa\sin\frac{s}{a} - \sin\Lambda. \quad \text{(A5)}$$

Incidentally, we can recover (A3) by letting $\kappa \to 0$ in (A5) and solving for $r$. Via a trigonometric identity (A5) becomes

$$\sin(\kappa r - \Lambda) = a\kappa\sin\frac{s}{a} - \sin\Lambda, \quad \text{(A6)}$$

so the formula for the slant range $r$ as a function of the ground range $s_\oplus$ and launch angle on the real Earth (case 4) is

$$r = \frac{1}{\kappa_\oplus}\left\{\alpha + \frac{s_\oplus}{a_\oplus} + \sin^{-1}\left[a_\oplus\kappa_\oplus\sin\frac{s_\oplus}{a_\oplus} - \sin\left(\alpha + \frac{s_\oplus}{a_\oplus}\right)\right]\right\}. \quad \text{(A7)}$$

For the flat earth with refraction (case 2), we change the subscripts in (A7) to $f$ and take the limit $a_f \to \infty$. This yields

$$r = \frac{1}{\kappa_f}[\alpha + \sin^{-1}(\kappa_f s_f - \sin\alpha)]. \quad \text{(A8)}$$

## REFERENCES


Askelson, M. A., 2002: Kinematic, dynamic, and thermodynamic impacts of hook-echo hydrometeors, including explorations into the utilization of polarimetric radar data. Ph.D. thesis, University of Oklahoma, 245 pp.

Davies-Jones, R., and V. T. Wood, 2006: Simulated Doppler velocity signatures of evolving tornado-like vortices. *J. Atmos. Oceanic Technol.*, **23**, 1029–1048, https://doi.org/10.1175/JTECH1903.1.

Doviak, R. A., and D. S. Zrnić, 2006: *Doppler Radar and Weather Observations*. 2nd ed. Dover, 562 pp.

Petrocchi, P. J., 1982: Automatic detection of hail by radar. Environmental Research Paper. 796, AFGL-TR-82-0277, Air Force Geophysics Laboratory, 33 pp.

Schelleng, J. C., C. R. Burrows, and E. B. Ferrell, 1933: Ultra-short-wave propagation. *Proc. Inst. Radio Engr.*, **21**, 427–463, https://doi.org/10.1109/JRPROC.1933.227639.

Stumpf, G., K. Hondl, S. B. Smith, R. Toomey, M. T. Filiaggi, and V. Lakshmanan, 2005: Status on the four-dimensional radar analysis tool for AWIPS. *11th Conf. on Mesoscale Processes/32nd Conf. on Radar Meteorology*, Albuquerque, NM, Amer. Meteor. Soc., P8R.4, https://ams.confex.com/ams/32Rad11Meso/webprogram/Paper96028.html.

Wood, V. T., R. Davies-Jones, and C. Potvin, 2018: Virtual near-radar Doppler velocity signatures of low-level supercell horizontal and vertical rotations: Simulation study. *29th Conf. on Severe Local Storms*, Stowe, VT, Amer. Meteor. Soc, 81, https://ams.confex.com/ams/29SLS/webprogram/Paper348096.html.

Xu, Q., and L. Wei, 2013: Prognostic equation for radar radial velocity derived by considering atmospheric refraction and earth curvature. *J. Atmos. Sci.*, **70**, 3328–3338, https://doi.org/10.1175/JAS-D-13-011.1.